VECTOR CONTROL FOR LINEAR INDUCTION MOTORS CONSIDERING END EFFECTS

Ezio Fernandes da Silva(Eng.)[1], Euler Bueno dos Santos(Dr.)[2] and Paulo César M. Machado(Ph.D.)[2]

[1]Centro Federal de Educação Tecnológica de Goiás - CEFET - GO
Rua 75 nº 46, Centro
74055-110 – Goiânia – Goiás - Brazil
efs@cefetgo.br

[2]Universidade Federal de Goiás
Escola de Engenharia Elétrica, s/n, Setor Universitário
74605-220 – Goiânia – Goiás - Brazil
ebs@eee.ufg.br

Abstract – **In this paper, a methodology for the vector control for linear induction motor by considering end effects is presented. A comparison with the conventional induction motor model is also performed.**

KEYWORDS
Linear Induction Motor, End Effect, Thrust, Vector Control.

I. INTRODUCTION

In recent years the vector control technique has been widely used in the way to allow that induction motor drivers result in high performance, such as that in the direct current.

The basic idea behind the vector control is uncoupling the flux and the torque of an induction motor, such as a torque response similar of a direct current machine is obtained. The flux orientation can be obtained by aligning the rotor flux vector with the reference d-axis, therefore becoming a highly coupled non-linear system dynamic control in a linear and uncoupled one.

The aim of the control oriented by the field is maintaining constant the d-axis rotor flux and making null the q-axis rotor flux.

The dynamic model of the linear induction motor (LIM) is analyzed by using the dq model of the equivalent electrical circuit with end effects included. A speed inverse function factor is determined to express the effects that the linear induction motor speed causes in the magnetization branch of the equivalent electrical circuit [1].

For a LIM with short primary and infinite linor, where the primary is movable and the linor is fixed, the primary will be continuously entering in a new linoric region. This new linoric region tends to oppose to the sudden increase in the penetration of the magnetization flux allowing a gradual accumulation of the magnetization field density in the air gap. The appearance of a new linoric region and its influence in the magnetic field modifies the LIM performance when compared to the conventional induction motor [2].

Figure 1 shows the linear induction motor used in this research, from which were obtained the parameter values given in table I.

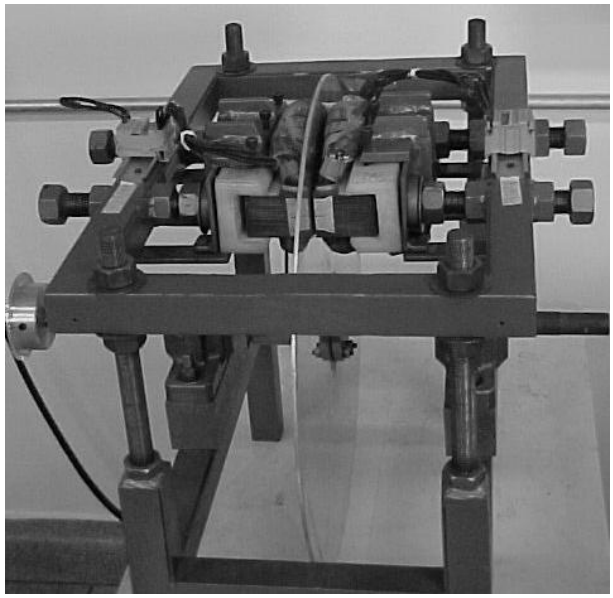

Figure 1 - Double face linear induction motor with linor (secondary) in aluminium disc.

The spatial distribution of the magnetic flux density along the width of the primary depends on the relative speed between primary and linor (secondary). For null speed of the primary, the LIM can be considered as having an infinite primary and in this case the end effects can be neglected.

II. LIM MATHEMATICAL MODEL

The q-axis equivalent circuit of the linear induction motor is identical to the q-axis equivalent circuit of the conventional induction motor, i.e. the parameters do not vary with the end effects.

However, the air gap flux is affected by the d-axis entry linoric currents. Therefore, the d-axis equivalent circuit of the conventional induction motor cannot be used in the linear induction motor analysis when the end effects are considered [1].

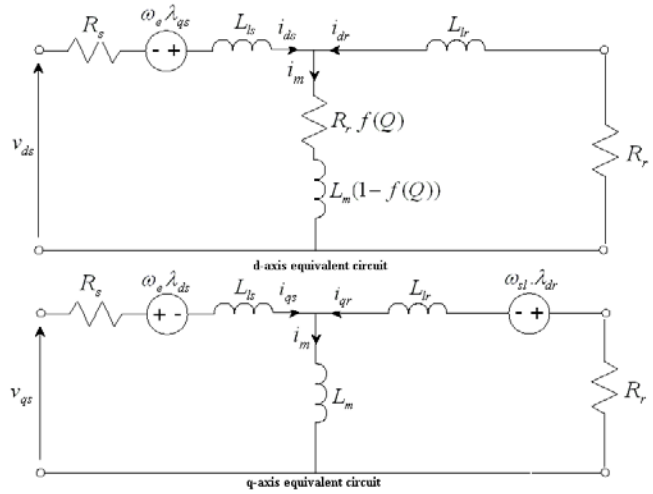

Figure 2 - dq equivalent circuit of the LIM including the end effects.

Figure 2(a) shows the d-axis equivalent circuit which magnetization branch is different from the conventional induction motor. In Figure 2 (b) the equivalent circuit is the same that the conventional induction motor.

From the dq equivalent circuit of the LIM (Fig. 2), the primary and linor voltage equations in a synchronous reference system (superscript "e") aligned with the linor flux are given by [1]:

$$v_{ds}^{e} = R_s i_{ds}^{e} + R_r f(Q)\left(i_{ds}^{e} + i_{dr}^{e}\right) + \frac{d\lambda_{ds}^{e}}{dt} - \omega_e \lambda_{qs}^{e} \quad (1)$$

$$v_{qs}^{e} = R_s i_{qs}^{e} + \frac{d\lambda_{qs}^{e}}{dt} + \omega_e \lambda_{ds}^{e} \quad (2)$$

$$v_{dr}^{e} = R_r i_{dr}^{e} + R_r f(Q)\left(i_{ds}^{e} + i_{dr}^{e}\right) + \frac{d\lambda_{dr}^{e}}{dt} = 0 \quad (3)$$

$$v_{qr}^{e} = R_r i_{qr}^{e} + \omega_{sl} \lambda_{dr}^{e} = 0 \quad (4)$$

where:

$$\lambda_{ds}^{e} = L_{ls} i_{ds}^{e} + L_m\left(1 - f(Q)\right)\left(i_{ds}^{e} + i_{dr}^{e}\right) \quad (5)$$

$$\lambda_{qs}^{e} = L_{ls} i_{qs}^{e} + L_m\left(i_{qs}^{e} + i_{qr}^{e}\right) \quad (6)$$

$$\lambda_{dr}^{e} = L_{lr} i_{dr}^{e} + L_m\left(1 - f(Q)\right)_m\left(i_{ds}^{e} + i_{dr}^{e}\right) \quad (7)$$

$$\lambda_{qr}^{e} = L_{lr} i_{qr}^{e} + L_m\left(i_{qs}^{e} + i_{qr}^{e}\right) \quad (8)$$

$$f(Q) = \frac{1 - e^{-Q}}{Q} \quad (9)$$

$$Q = \frac{DR_r}{\left(L_m + L_{lr}\right)v} \quad (10)$$

where $v_s = v_{ds} + jv_{qs}$ is the primary voltage, $v_r = v_{dr} + jv_{qr}$ the linor voltage, $L_s = L_{ls} + L_m$ the primary inductance, $L_r = L_{lr} + L_m$ the linor inductance, L_{ls} the primary leakage inductance, L_{lr} the linor leakage inductance, and L_m the magnetizing inductance. Subscripts "s" and "r" denote the primary and linor values, respectively. Subscripts d and q denote d-axis and q-axis values, respectively. v_{ds}, v_{qs} are the primary voltages; v_{dr}, v_{qr} the linor voltages; i_{ds}, i_{qs} the primary electrical currents; i_{dr}, i_{qr} the linor electrical currents; $\lambda_s = \lambda_{ds} + j\lambda_{qs}$, $\lambda_r = \lambda_{ds} + j\lambda_{qr}$ the primary and linor linkage flux; R_s, R_r the primary and linor resistances; ω_{sl} the slip frequency; P the pole number; v the linear speed in m/s; D the primary length in meters; Q is a factor related to the primary length, which quantifies the end effects as a function of the speed (v).

It can be seen in (10) that the Q factor depends on the inverse of the speed, i.e. for null speed the primary length can be considered infinite and, therefore, the end effects can be neglected.

One can see that the primary length decreases with increasing speed, therefore increasing the end effects. It will reduce the magnetization current of the LIM. This effect can be quantified by modifying the magnetization inductance.

The resistance inserted in series with the inductance $L_m\left(1 - f(Q)\right)$ in the magnetization branch of the d-axis equivalent electrical circuit is determined from the increase of the loss with increasing linor inducted electrical currents in the entry and exit. These power losses can be represented by the linor resistance times the $f(Q)$ factor, i.e. $R_r f(Q)$, serially connected in the d-axis magnetizing current branch [1][2].

The thrust is given by:

$$F_e = \frac{3\pi}{2\tau_p}\frac{P}{2}\left(\lambda_{ds}^{e} i_{qs}^{e} - \lambda_{qs}^{e} i_{ds}^{e}\right) \quad (11)$$

III. VECTOR CONTROL FOR LIM

The vector control for LIM can be analyzed in the same way as the conventional induction motor. One problem in the LIM case is that a new resistance and inductance, which are speed dependent, are included in the magnetization branch. This will difficult the flux and thrust decoupling.

In this paper the parameter variations are neglected. However, new research will be carried out to develop new techniques that include parameter variations.

A. Slip speed

In order to determine the slip angular speed, the linor q-axis flux must be considered zero $\left(\lambda_{qr}^{e} = 0\right)$. Then, the linor q-axis electrical current can be determined from (8) giving the

following equation:

$$i_{qr} = -\frac{L_m . i_{qs}}{L_r} \tag{12}$$

From (4) one can obtain the slip frequency :

$$\omega_{sl} = -\frac{R_r i^e_{qr}}{\lambda^e_{dr}} \tag{13}$$

Replacing (12) in (13) it is obtained:

$$\omega_{sl} = -\frac{R_r i^e_{qr}}{\lambda^e_{dr}} = \frac{1}{T_r}\frac{L_m}{\lambda^e_{dr}} i^e_{qs} \tag{14}$$

where $T_r = L_r / R_r$ is the linor time constant.

The slip frequency equation ω_{sl} is the same that the conventional induction motor. The main difference is the characteristic λ^e_{dr}.

i^e_{dr} can be obtained from (3):

$$i^e_{dr} = -\frac{\frac{d\lambda^e_{dr}}{dt} + R_r f(Q) i^e_{ds}}{R_r[1 + f(Q)]} \tag{15}$$

Replacing (15) in (7) one can obtain:

$$\frac{d\lambda^e_{dr}}{dt}[L_m - L_r f(Q)] + \lambda^e_{dr} R_r [1 + f(Q)] = R_r i^e_{ds}[L_m - L_r f(Q)] \tag{16}$$

λ^e_{dr} is obtained from (16):

$$\lambda^e_{dr} = \frac{(L_m - L_r f(Q)) R_r i^e_{ds}}{p[L_m - L_r f(Q)] + R_r[1 + f(Q)]} \tag{17}$$

where p is the differential operator representation d/dt.

If we consider constant linor flux in (17), we can obtain:

$$\lambda^e_{dr} = \frac{(L_m - L_r f(Q)) i^e_{ds}}{1 + f(Q)} \tag{18}$$

Replacing (18) in (14), we obtain:

$$\omega_{sl} = \frac{i_{qs}(1 + f(Q))}{T_r . i_{ds}\left(1 - f(Q)\frac{L_r}{L_m}\right)} \tag{19}$$

For a LIM in low speed operation, i.e. for $f(Q)$ approximately zero in (19), one can obtain an equation to the slip frequency similar to the used for the vector control of the conventional induction motor.

The slip frequency ω_{sl}, which depends on the rotor time constant and $f(Q)$, can be determined from (19). However, linor resistance variations can make it difficult to obtain the linor and thrust decoupling.

Several control strategies have been elaborated in order to obtain a vector control that does not depend on the parameter variations.

The primary angular frequency can be determined by adding the linor angular speed with the slip frequency. This will give us:

$$\omega_e = \omega_r + \omega_{sl} \tag{20}$$

The transformation of the linear speed of the LIM to an angular speed is given by:

$$\omega_r = \frac{\pi}{\tau_p} v \tag{21}$$

where: ω_r represents the linor angular speed and τ_p is the step polar, which is given by $\tau_p = D/P$. From the knowledge that $\omega_e = d\theta_e / dt$, the linor flux position angle related to the primary can be determined by :

$$\theta_e = \int \omega_r . dt + \int \omega_{sl} . dt \tag{22}$$

The linor flux instantaneous position angle has to be used in the transformation of the stationary reference systems to synchronous and vice-versa, as can be seen in the block diagram of the vector control in Figure 3.

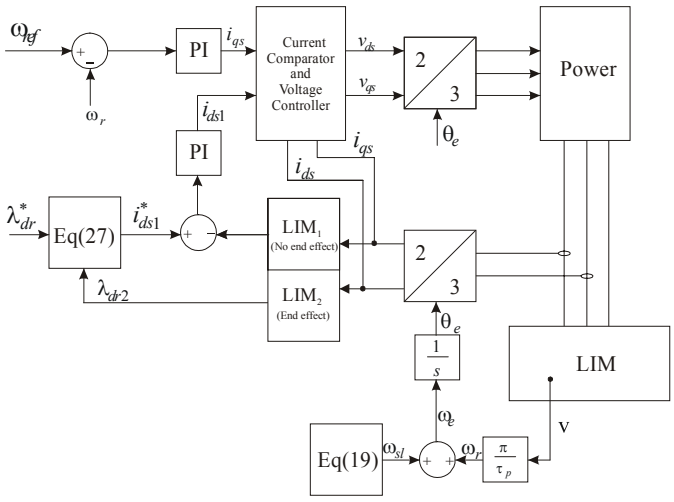

Figure 3 - Block diagram of the vector control for LIM

B. Determination of the primary reference electrical current.

The aim of the vector control is obtaining the linor flux and thrust decoupling. Therefore a constant steady-state linor flux is necessary.

The linor flux can be separated in two parts as can be seen in the appendix. The "1" index parts are independent of the extremities effects and the "2" index parts are dependent of the end effects. The linor flux has to be considered constant, therefore (17) can be rewritten as:

$$\lambda^e_{dr} = \frac{(L_m - L_r f(Q)) i^e_{ds}}{1 + f(Q)} = \lambda^e_{dr1} + \lambda^e_{dr2} \tag{23}$$

where:

$$i^e_{ds} = i^e_{ds1} + i^e_{ds2} \tag{24}$$

Replacing (24) in (23) one can obtain (25) after some mathematical manipulations.

$$\lambda^e_{dr1} = L_m . i^e_{ds1} \tag{25}$$

$$\lambda^e_{dr2} = L_m i^e_{ds2} + \frac{(L_m - L_r f(Q)) i^e_{ds}}{1 + f(Q)} \tag{26}$$

From (26), it can be seen that the linor d-axis flux (index "2") is a function of i_{ds1}, i_{ds2} and $f(Q)$, where i_{ds1} is a

control variable.

In order to obtain the control current $\left(i_{ds1}^{e}\right)$, by maintaining constant the linor reference flux $\left(\lambda_{dr}^{e*}\right)$, equation (27) has to be considered:

$$i_{ds1}^{e*} = \frac{\lambda_{dr}^{e*} - \lambda_{dr2}^{e}}{L_m} \tag{27}$$

The primary reference current $\left(i_{ds1}^{e*}\right)$ is applied to a PI controller as seen in Figure 3.

IV. VECTOR CONTROL SIMULATION FOR LIMs

The LIM values used in the dynamic simulation are shown in Table I.

TABLE I
Linear Induction Motor Values

LIM –1	
Data	**Values (Unit)**
Primary length - D	210 mm
Primary width	45 mm
Pole number - P	2
Pole pitch	98.5 mm
Slot number	12
Linor thickness	4.5 mm
Air gap length	10 mm
Primary resistance - R_s	5.348 Ω
Linor resistance - R_r	11.603 Ω
Primary inductance - L_s	0.1073 mH
Linor inductance - L_r	0.094618 mH
Magnetizing inductance - L_m	0.09213 mH
Inertia moment – J	0.00247 Kgm^2

Figure 4 shows a SIMULINK block diagram of the vector controller. In the simulation, the following values were used: a 2 m/s velocity reference signal at 0.1 s, and a load of 60 N applied in the [0.3, 0.4] second interval. Figure 5 shows the thrust response obtained with the above reference signal values. The d-axis linor flux should be constant and equal to the reference linor flux of 0.5 Wb. Instead, as shown in figure 6, a small disturbance occurred soon after the reference velocity and load were applied. A PI controller was used to obtain the linor flux values shown, which are considered satisfactory. The q-axis flux shown in figure 7 has a near-zero value, which is a satisfactory response for the vector control. Figure 8 shows the reference velocity and the actual velocity attained by the LIM, where one may note that even with the application of the load in the [0.3, 0.4] second interval, the resulting velocity disturbance was small, which is a very satisfactory result. Figure 9 shows the d-axis and q-axis primary currents, while figure 10 shows the current of one phase applied to the LIM. In Figure 11 we have a comparison between the d-axis linor fluxes for two cases of reference velocity values: 2 m/s and 5 m/s. Note that, for the higher velocity the disturbances are more marked, due to the increased extremity effects appearing at higher speeds.

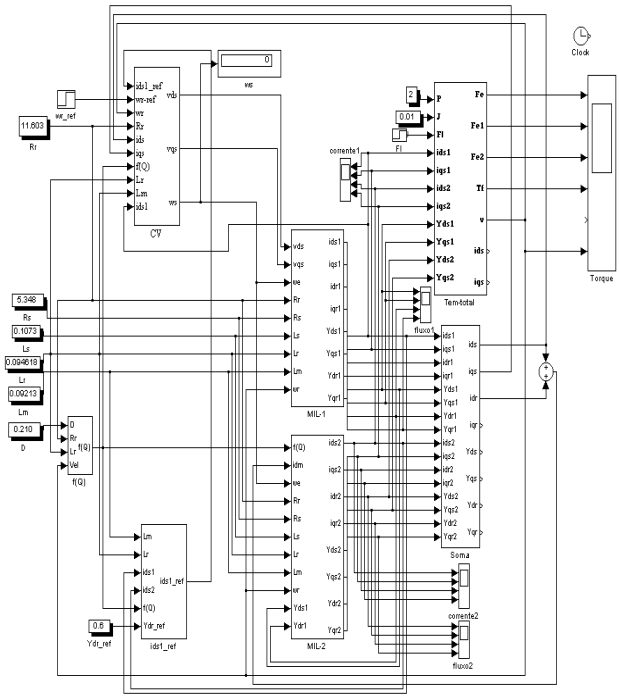

Figure 4 - Simulation diagram of the vector control for LIM by using the SIMULINK.

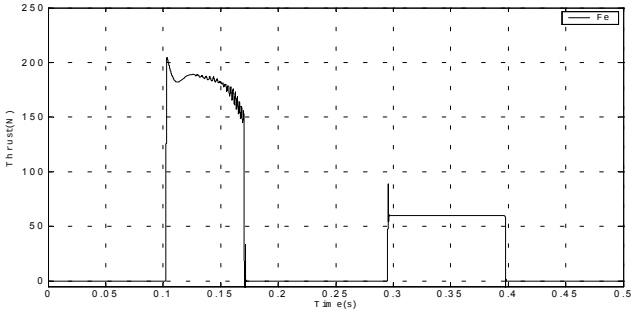

Figure 5 - Thrust simulation F_e.

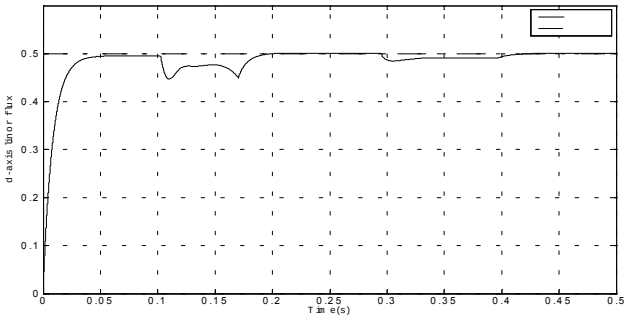

Figure 6 - Simulation: Linor d-axis flux λ_{dr}^{e} (solid line) and linor flux reference λ_{dr}^{e*} (dashed line) of 0,5 Wb for the speed reference to 2 m/s

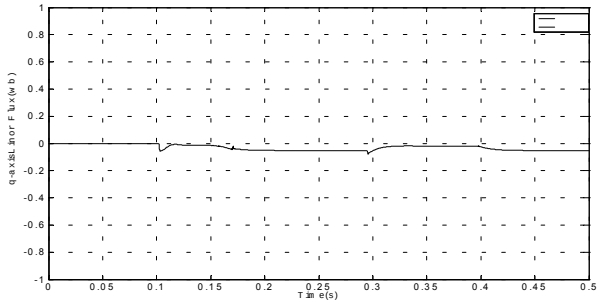

Figure 7 - q-axis linor flux simulation

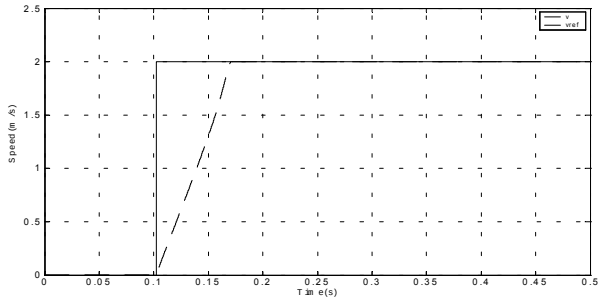

Figure 8 – Simulation: Linor speed ν (solid line) and speed reference (dashed line) of 2 m/s.

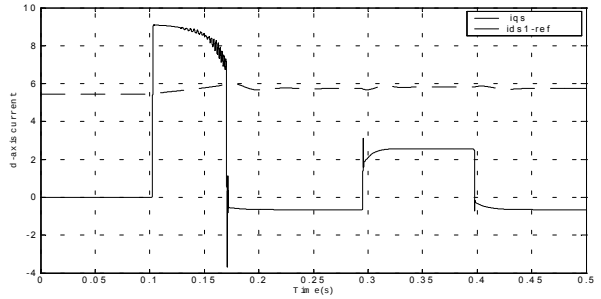

Figure 9 - d-axis primary current of "1" index (solid line) and q-axis primary current (dashed line).

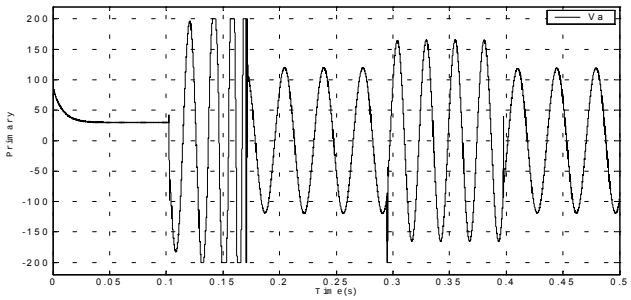

Figure 10 - Current simulation of a LIM primary phase

Changing the speed reference to 5 m/s, one can verify that the d-axis linor flux becomes less than the speed reference of 2 m/s, due to the increasing of the end effects caused by the increased speed as shown in Figure 11.

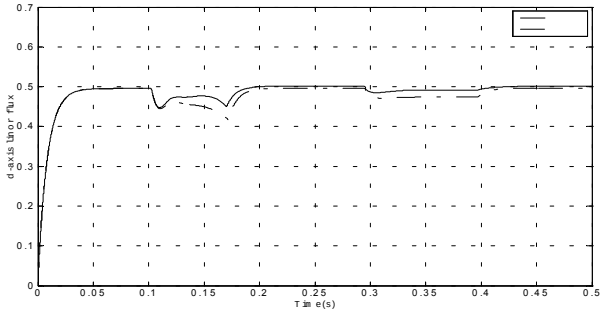

Figure 11 - Simulation: Linor d-axis flux (solid line) for the speed reference to 2 m/s and (dashed line) for the speed reference to 5 m/s.

V. CONCLUSIONS

As a first step in studying the vector control for LIM by using vector control techniques, we have obtained good results in comparison with what has been predefined.

In order to have a good vector control the d-axis linor flux graphics must be constant in relation to the preset reference. However, the q-axis linor flux would be zero. Small variations in the linor flux were observed as shown in Figures 6 and 7. These variations come from the end effects.

One can observe that the end effects become more accentuated with increasing speed, as can be seen in Fig. 11.

Equations (19) and (27) were used in the LIM vector control and they have worked very well in relation to the speed reference and strength load reference as can be seen in Figures 8 and 5, respectively.

It can be seen that in spite of the small d- and q-axis linor flux variation, the responses have been maintained without suffering from oscillations maintaining the high performance proposed by the vector control.

We point out that new methodologies are been studied in order to consider the parameter variations and minimize the linor flux variations.

VI. APPENDIX

A. Separating the dq Primary Currents from the Linor Current

The d- and q-axis primary currents and linor current of the LIM can be determined after some mathematical manipulation of the equations (1) to (8), and it is obtained:

$$i_{ds}^{e} = \frac{\left(L_r - L_m f(Q)\right)\lambda_{ds}^{e} - L_m\left(1 - f(Q)\right)\lambda_{dr}^{e}}{\left(L_s - L_m f(Q)\right)\left(L_r - L_m f(Q)\right) - L_m^2\left(1 - f(Q)\right)^2} \quad \text{(A.1)}$$

$$i_{dr}^{e} = \frac{\left(L_s - L_m f(Q)\right)\lambda_{ds}^{e} - L_m\left(1 - f(Q)\right)\lambda_{ds}^{e}}{\left(L_s - L_m f(Q)\right)\left(L_r - L_m f(Q)\right) - L_m^2\left(1 - f(Q)\right)^2} \quad \text{(A.2)}$$

The dq primary currents and linor current of the LIM can be separated in two parts, where the first one is independent

from the end effects and the second one is dependent from this effect. The first part behaves as a conventional induction motor current and the second part represents a function of the attenuation that exists in the LIM due to the end effects.

In order to obtain these currents, it has to be considered that the linkage flux is separated into two parts: the first refers to the linkage flux that is independent of the end effects and it will be denoted by the "1" index. The second part refers to the linkage flux that is dependent from the end effects and it will be denoted by the "2" index. These fluxes are obtained from the following equations:

$$\lambda_{ds}^{e} = \lambda_{ds1}^{e} + \lambda_{ds2}^{e} \quad (A.3)$$

$$\lambda_{qs}^{e} = \lambda_{qs1}^{e} + \lambda_{qs2}^{e} \quad (A.4)$$

$$\lambda_{dr}^{e} = \lambda_{dr1}^{e} + \lambda_{dr2}^{e} \quad (A.5)$$

$$\lambda_{qr}^{e} = \lambda_{qr1}^{e} + \lambda_{qr2}^{e} \quad (A.6)$$

Inserting the equations (A.3 to A.6) in (A.1 to A.2), and after some mathematical manipulations one can obtain the following expressions:

$$i_{ds}^{e} = i_{ds1}^{e} + i_{ds2}^{e} \quad (A.7)$$

$$i_{qs}^{e} = i_{qs1}^{e} + i_{qs2}^{e} \quad (A.8)$$

$$i_{dr}^{e} = i_{dr1}^{e} + i_{dr2}^{e} \quad (A.9)$$

$$i_{qr}^{e} = i_{qr1}^{e} + i_{qr2}^{e} \quad (A.10)$$

where:

$$i_{ds1}^{e} = \frac{L_r \lambda_{ds1}^{e} - L_m \lambda_{dr1}^{e}}{L_\sigma} \quad (A.11)$$

$$i_{dr1}^{e} = \frac{L_s \lambda_{dr1}^{e} - L_m \lambda_{ds1}^{e}}{L_\sigma} \quad (A.12)$$

$$i_{ds2} = A_1 + A_2 + A_3 \quad (A.13)$$

$$A_1 = \frac{L_r \lambda_{ds2} - L_m \lambda_{dr2}}{L_\sigma} \quad (A.14)$$

$$A_2 = \frac{L_m L_l f(Q)\left(L_r \lambda_{ds} - L_m \lambda_{dr}\right)}{L_\sigma \left(L_\sigma - L_m L_l f(Q)\right)} \quad (A.15)$$

$$A_3 = \frac{L_m L_\sigma f(Q)(\lambda_{ds} - \lambda_{dr})}{L_\sigma \left(L_\sigma - L_m L_l f(Q)\right)} \quad (A.16)$$

$$i_{dr2} = A_4 + A_5 + A_6 \quad (A.17)$$

$$A_4 = \frac{L_s \lambda_{dr2} - L_m \lambda_{ds2}}{L_\sigma} \quad (A.18)$$

$$A_5 = \frac{L_m L_l f(Q)\left(L_s \lambda_{dr} - L_m \lambda_{ds}\right)}{L_\sigma \left(L_\sigma - L_m L_l f(Q)\right)} \quad (A.19)$$

$$A_6 = \frac{L_m L_\sigma f(Q)(\lambda_{dr} - \lambda_{ds})}{L_\sigma \left(L_\sigma - L_m L_l f(Q)\right)} \quad (A.20)$$

$$i_{qs1}^{e} = \frac{L_r \lambda_{qs1}^{e} - L_m \lambda_{qr1}^{e}}{L_\sigma} \quad (A.21)$$

$$i_{qs2}^{e} = \frac{L_r \lambda_{qs2}^{e} - L_m \lambda_{qr2}^{e}}{L_\sigma} \quad (A.22)$$

$$i_{qr1}^{e} = \frac{L_s \lambda_{q1s}^{e} - L_m \lambda_{qs1}^{e}}{L_\sigma} \quad (A.23)$$

$$i_{qr2}^{e} = \frac{L_s \lambda_{q2s}^{e} - L_m \lambda_{qs2}^{e}}{L_\sigma} \quad (A.24)$$

$$L_\sigma = L_s L_r - L_m^2 \quad (A.25)$$

$$L_l = L_{ls} + L_{lr} \quad (A.26)$$

B. Separating the Linkage Flux.

The linkage flux can be obtained from the following differential equations:

$$\frac{d\lambda_{ds1}^{e}}{dt} = v_{ds}^{e} - R_s i_{ds1}^{e} + \omega_e \lambda_{qs1}^{e} \quad (B.1)$$

$$\frac{d\lambda_{ds2}^{e}}{dt} = -R_s i_{ds2}^{e} + \omega_e \lambda_{qs2}^{e} - R_r f(Q)\left(i_{ds}^{e} + i_{dr}^{e}\right) \quad (B.2)$$

$$\frac{d\lambda_{qs1}^{e}}{dt} = v_{qs}^{e} - R_s i_{qs1}^{e} - \omega_e \lambda_{ds1}^{e} \quad (B.3)$$

$$\frac{d\lambda_{qs2}^{e}}{dt} = -R_s i_{qs2}^{e} - \omega_e \lambda_{ds2}^{e} \quad (B.4)$$

$$\frac{d\lambda_{dr1}^{e}}{dt} = -R_r i_{dr1}^{e} + \omega_{sl} \lambda_{qr1}^{e} \quad (B.5)$$

$$\frac{d\lambda_{dr2}^{e}}{dt} = -R_r i_{dr2}^{e} + \omega_{sl} \lambda_{qr2}^{e} - R_r f(Q)\left(i_{ds}^{e} + i_{dr}^{e}\right) \quad (B.6)$$

$$\frac{d\lambda_{qr1}^{e}}{dt} = -R_r i_{qr1}^{e} - \omega_{sl} \lambda_{dr1}^{e} \quad (B.7)$$

$$\frac{d\lambda_{qr2}^{e}}{dt} = -R_r i_{qr2}^{e} - \omega_{sl} \lambda_{dr2}^{e} \quad (B.8)$$

REFERENCES

[1] K.Nam, J. H Sung, "A New Approach to Vector Control for Linear Induction Motor Considering End Effects" IEEE IAS annual meeting, 3-7 Oct., in Phoenix, Arizona, pp. 2284-2289, 1999.

[2] J. Duncan, "Linear Induction Motor – Equivalent Circuit Model". IEE Proc., Vol. 130, pt. B, nº 1, pp. 51-57, January, 1983.

[3] E.B. Santos, J.R. Camacho, A.A. Paula, "The Linear Induction Motor (LIM) Power Factor, Efficiency and Finite Element Considerations.", ICEM 2002, CD-ROM.

[4] L.M. Neto, E.B. Santos, "Métodos para Determinação de Indutâncias de um Motor de Indução Linear", Anais do Congr. Brasil. de Automática - Uberlândia-MG, v. 1, pp. 231-236, 2000.

[5] J.F. Gieras, "Linear Induction Drives", University of Tokyo Press, Japan, 1994.

[6] R.C. Creppe, "Uma contribuição à modelagem de Máquinas de Indução Lineares", Tese de Doutorado, UNICAMP, Campinas, São Paulo, Brasil, 1997.